Investigating Small-Scale Terrain and Meteorological Influences on Atmospheric CO_2

ATM OCN 404: Meteorological Measurements

Sophie Hoffman, Peter Janssen, James Mineau, Iman Nasif, Juliet Pilewskie, Jess Turner

---

Abstract

Natural variation in atmospheric carbon dioxide concentrations is influenced by synoptic events, time of day, wind speed, and surface temperature. This study was an attempt to observe how concentrations of CO_2 (ppm) varied across regions of different ecological characteristics, while also monitoring the meteorology of each terrain. This experiment was conducted during the first Intensive Operation Period of the Chequamegon Heterogeneous Ecosystem Energy-balance Study Enabled by a High-density Extensive Array of Detectors (CHEESEHEAD) field campaign as part of the Meteorological Measurements course at UW-Madison. Our group measured CO_2 concentrations at the surface and recorded wind speed and boundary layer height at time of measurement. Initial measurements were taken in a mowed grass field, with a second launch performed downwind where measurements were taken at different locations each day in an attempt to capture large-scale eddies as they moved across the landscape. Results showed that the largest increase in downwind CO_2 concentration from the starting location was alongside a long and narrow lake, but the smallest differences were noted near a round lake and at a campground built near rapids.

1. Introduction

The Chequamegon Heterogeneous Ecosystem Energy-balance Study Enabled by a High-density Extensive Array of Detectors (CHEESEHEAD) project is a three-month field campaign held in a 10x10 kilometer area of the Chequamegon National Forest in Park Falls, Wisconsin. The focus of CHEESEHEAD is to address the way the atmospheric boundary-layer responds to scales of spatial heterogeneity in the lower and surface-atmosphere heat and water exchanges, yet the campaign is also involved in various other scientific applications such as gathering numerical meteorological data and forestry and ecological properties of the land.

The purpose of this experiment was to measure the movement of carbon dioxide over various terrains and landscapes. To measure this, we developed an experiment that would allow for tracking CO_2 between two locations. Following the initial windsonde launch, we were able to use wind speed and direction to estimate an approximate second location (Figures 15-24). Upon calculating the second location, we were able to navigate to our second launch site. CO_2 measurements were recorded at each launch site, as well as during navigation from the first site to the second site. Foliage and terrain were also observed during navigation to later analyze possible effects on our CO2 recordings.

1.1 Background

With global concentrations of CO_2 increasing annually, CO_2 fluxes and transport mechanisms are being studied in a plethora of regions and synoptic conditions. The site of the CHEESEHEAD project as well as the WLEF 447m Tall Tower have been used over the past couple of decades to study CO_2 and what factors impact its movements & concentration.

In a study predating CHEESEHEAD, archival mixing ratio data from the WLEF Tall Tower was utilized to observe large fluctuations in CO_2 between the years 1998 and 2000. At the time of this study, WLEF collected data every twelve minutes, making large changes in CO_2 mixing ratios easily detectable. Large fluctuations in CO_2 mixing ratio generally occurred simultaneously with a large fluctuation in temperature or water mixing ratio, or lined up with incoming or outgoing frontal movements. This led to the observation that CO_2 concentrations in an area are heavily influenced by frontal movements and synoptic events (Hurwitz et al. 2004).

Surface CO_2 fluxes experience strong diurnal and seasonal cycles in mid-latitude forests due to both biological and advective mixing processes. At night, high mixing ratios are expected in the stable boundary layer as soil microbes and plants respire. After sunrise, CO_2 becomes well mixed due to the boundary layer deepening, and the boundary layer deepening slows down the rate of change of CO_2 mixing ratios (Bakwin et al. 1998; Yi et al. 2001; Davis et al. 2003). Photosynthesis exceeds respiration at the surface, which causes CO_2 concentration to decrease throughout the day. The average daytime value of surface CO_2 fluxes is negative during the growing season (late May-early September) due to photosynthesis. Other times of the year, the fluxes are positive as respiration exceeds photosynthesis. Yet, it is possible for the sign of the surface CO_2 fluxes to differ from the change in CO_2 concentrations, which means that the horizontal and/or vertical transport of CO_2 are important contributions to changing CO_2 concentrations (Davis et al. 2003).

By combining the WLEF mixing ratio and exchange data with tower data from the Harvard Forest Environmental Measurement Site in Massachusetts, a section of the BOREAS Northern Study Area in Manitoba, Canada, and a tower site in Hungary, it was deemed possible to measure the net ecosystem exchange. With all sites in comparable climates and ecosystems, diurnal CO_2 fluctuations were observed and budgets were calculated. Similar observations were taken regarding frontal movements. Through analyzing previously calculated budgets, researchers concluded calculating average surface flux is possible on a regional scale with the proper grid setup (P.S. Bakwin et al. 2004).

Most recently, CO_2 variations were simulated after filtering through cold fronts recorded in WLEF data. From 1997 to 2001, 12 out of 51 cold fronts were selected to be simulated in a program utilizing the Regional Atmospheric Modeling System (RAMS) as well as SIB 2.5 in lieu of LEAF (Land Ecosystem-Atmosphere Feedback). The model, which simulated a full atmosphere-biosphere complete with photosynthesis prediction, showed that CO_2 variations are influenced by horizontal advection in addition to local land surfaces and transport processes (Wang et al. 2007).

1.2 Questions and Hypotheses

The goal of this experiment was to answer the following questions: What is the influence and significance of varying ecological characteristics (surface heterogeneity) on atmospheric CO_2 concentrations? How might meteorology influence atmospheric CO_2?

We hypothesize that one of the following will be true:

- CO_2 concentrations will not vary across terrain, **OR**
- CO_2 concentrations will vary across terrain due to meteorology, **OR**
- CO_2 concentrations will vary across terrain but largely due to vegetation.

2. Methods & Instrumentation

In order to focus on variability due to terrain and other meteorological factors, all measurements, including CO_2 concentrations, were taken within a specific study region and similar time frame daily. The initial windsonde launch and CO_2 concentration measurements took place between 9:00-10:30 AM CDT each day at the ISS (Integrated Sounding System) field, located east of the WLEF tall tower and centrally within the CHEESEHEAD domain. Picarro GasScouter concentration data was collected for ~15 minutes during each launch period. The windsonde was allowed to reach the boundary layer while continuously taking measurements before being cut for retrieval. The location of the second windsonde launch varied daily and was determined by wind direction and land accessibility in order to measure downwind CO_2 concentrations (Figure 1). These secondary launches and downwind concentration measurements were completed in the late morning--always before 12:00 PM CDT.

The vegetation data was received as plots of the National Forest and local private lands from the U.S. Forest Service. Then overlaying a straight line between the initial Picarro location and final location (Figure 2), points were created at every 50 meters from the start and attributed to the vegetation at that point with ArcGIS Pro (Figure 3). This is an assumed path and the vegetation represented is the dominant species or type at that point. This method assumes that the air parcel traveled in a straight line through generalized vegetation.

2.1 Instrumentation

The chief instruments used in this study were windsondes and the Picarro GasScouter™ G4301 Mobile Gas Concentration Analyzer. Picarro near-surface measurements were recorded at 1 Hz. Related datasets and observations from the CHEESEHEAD field campaign were also made available to support this team's research. This included CO_2 flux and concentration (in ppm) measurements recorded by the WLEF Tall Tower, in close proximity of the daily initial windsonde launch point. Data from the WLEF tall tower was used for comparison to Picarro measurements and for meteorological data. Tall tower data is recorded at 10 Hz.

The primary utility of the windsondes was to provide an accurate wind direction and boundary layer height from its low-level atmospheric profile. Analogous to a typical radiosonde device, the windsonde tracks meteorological variables including wind speed & direction, temperature, pressure, relative humidity and altitude. These variables were tracked in real-time using a Panasonic Toughbook. The components of the sonde are housed within a small styrofoam cup with a plastic lid making it reasonably waterproof. The windsonde is also equipped with a GPS beacon that sends its coordinates to the receiver, which facilitates possible sonde retrieval.

The Picarro GasScouter™ analyzes multiple greenhouse gas concentrations including the variable our team was most interested in, carbon dioxide (CO_2). The instrument is entirely self-contained utilizing lasers, vacuum pumps and a central processing unit for data collection. The GasScouter™ provides accurate high-frequency CO_2 concentration measurements (in ppm), recording concentrations once every second.

2.2 Wavelet Analysis

Tall tower data was averaged every 10 values in order to compare to Picarro measurements. Picarro measurements at the second location were compared to WLEF tall tower 396 m concentrations at the time when the same wind measured by the Picarro would have theoretically passed over ISS. The traveling time for theoretical wind, or a large eddy, to move from ISS to the second location was calculated by dividing the distance between the two locations by mean wind speed (taken from initial windsonde launch at ISS). Times with missing tall tower data were removed from both datasets in order to create a finite data series for the wavelet.

The duration and 1 Hz frequency of Picarro measurements (as opposed to 10 Hz at WLEF) was a limitation. Larger eddies or storms that took place outside of the time of observation would not be displayed on the wavelet. In order to verify that correlations were due to CO_2 traveling from the upwind site to the downwind site, and were not artefacts of incoming solar radiation or meteorological conditions that would have impacted both sites, we created a wavelet comparing CO_2 concentration data from the downwind Picarro to upwind WLEF from the same time frames. The comparison revealed that there was a correlation between upwind WLEF and downwind Picarro measurements on Day 1, even without a time lag. However, this correlation was only noted at high frequencies. Wavelets are shown in Figures 4-8 in the appendix.

2.3 Boundary Layer Detection

Boundary layer depth influences CO_2 mixing ratios; as the boundary layer depth increases, CO_2 concentrations decrease because there is a larger volume to fill. Because the height of the boundary layer changes throughout the day, the rate of change of CO_2 mixing ratios does so as well. Thus, surface CO_2 flux calculations are dependent upon the height of the boundary layer. Vertical profiles of potential temperature, relative humidity, and wind speed --created with windsonde data--were used to qualitatively assess the height of the boundary layer at each measurement site. The straightforward way for detecting the boundary layer height was by looking for an inversion in potential temperature. Other methods used included finding the height of the minimum vertical gradient in relative humidity and a large gradient in wind speed. Figure 9 shows potential temperature profiles from Field Day 5 (7-13-19) with the boundary layer heights (marked in red) evident by the inversions.

The boundary layer heights from each site were averaged and used in calculating the surface fluxes of CO_2 with the equation

$$F = \frac{Cout - Cin}{\Delta t} \cdot z_i$$

(1)

where C_{in} and C_{out} are the atmospheric CO_2 concentrations measured by the Picarro at the first and second sites, respectively. The change in time between measurements is represented by Δt, and the boundary layer height is z_i. We ignored entrainment by not accounting for the differences in boundary layer heights between each measurement site.

3. Results

3.1 Vegetation Types and Deviation of Ground Level CO_2

Figure 3 in the appendix shows vegetation cover types between the first and second launch sites. On Day 1, land cover between ISS and Hay Lake was mainly aspen but there was also a large amount of open lowlands (Figure 9). The lowest standard deviation (3.7) and range of ground-level CO_2 concentrations (383.2,416.2 ppm) compared to other second launch locations were found at Hay Lake. On Day 2, dominant vegetation between ISS and Newman Springs was aspen and hardwoods (Figure 10). The standard deviation (10.5) and range of CO_2 concentrations (398.7, 732.0 ppm) were similar to other days. On Day 3, the dominant vegetation between ISS and Wintergreen Lake was aspen and lowland conifer (Figure 11). This location also had the largest standard deviation (28.9) and range of CO_2 concentration (398.7,732.0 ppm) compared to all other second launch locations. On Day 4, the dominant vegetation between ISS and Patterson Lake was red pine (Figure 12). The standard deviation (11.7) and range (393.4, 514.2 ppm) of CO_2 concentration were similar to other days. On Day 5, the dominant vegetation between ISS and Smith Rapids was aspen (Figure 13). The standard deviation (15.5) and range (374.1, 555.6 ppm) of CO_2 concentrations were higher than most other days.

3.2 Wavelet Analysis

Coherence was noted between upwind and downwind CO_2 concentrations even without using a time lag on Day 1. However, the wavelets created using a time lag (Figures 4-8) displayed low-frequency coherence that was not found when comparing upwind and downwind data taken at the same time. Wavelets from all days show high coherence between CO_2 concentrations at the first and second sites at the low frequency of 4-8 mHz when using the calculated travel time for large eddies as a lag. However, the duration of coherence at this frequency was very short (as low as one minute).

3.3 Meteorological Impact on CO_2 Fluxes

Temperature, relative humidity, and wind speeds were relatively consistent between each day, yet the synoptic conditions varied. Day one had clear conditions with a shallow inversion in the boundary layer at the times of our windsonde launches as shown in Figures 25-26. Day two was marked with a cold front passing over in the morning with a well-mixed boundary layer (Figures 27-28). Both days three and five were in the wake of a cold front with well-mixed boundary layers (Figures 29-30 and 9). And day four was in the onset of a storm with a shallow inversion in the atmospheric boundary layer (Figures 31-32).

In order to distinguish the concentration of CO_2 due to vegetation, surface CO_2 fluxes were calculated with the Picarro CO_2 concentrations using Equation 1 for each campaign day. Table 1 in the appendix shows average boundary layer heights, CO_2 fluxes calculated from Picarro data, and eddy fluxes provided by the WLEF Very Tall Tower. Days one and three have exceptionally large positive CO_2 surface flux values from the Picarro measurements, which corresponds to a carbon source at the surface. This is in contrast to negative WLEF eddy flux value at 122 m, which denotes a sink at the surface. Days two and four have smaller yet positive CO_2 surface flux values, which still contrasts to the negative WLEF eddy flux value on day two and the small positive value on day four. The surface flux of CO_2 for day five is different from the other days because it is negative, which indicates a carbon sink like the WLEF measurement, but it is much larger in magnitude than the flux measured by WLEF.

Despite a well-mixed boundary layer, day three had one of the largest surface CO_2 fluxes of our field campaign. It is possible that the low relative humidity influenced the large surface CO_2 fluxes seeing that these are indirectly proportional to each other (Hurwitz et al. 2002). The boundary layer was not well-mixed for days one, four, and during the launch at ISS for day five. For each of these days there are drastically different surface CO_2 flux values calculated using the Picarro measurements. This signifies the presence of weak mixing, which allows for strong vertical gradients of CO_2.

4. Discussion

4.1 Ground Level CO_2 and Vegetation Type

Aspen was one of the main vegetation types for each day except Day 4. It is interesting to note that lowland conifer was one of the main land cover types, in addition to aspen, when CO_2 concentration showed the largest increase relative to ISS. The second largest increase in CO_2 was when the path between first and second measurements included a large amount of open lowlands. Perhaps there were fewer trees to absorb CO_2 along the path, which allowed CO_2 to accumulate instead.

4.2 Wavelet Analysis

The wavelet analysis in Figures 4-8 (See Appendix) shows that WLEF measurements at 396 m were correlated with measurements at the second location after a certain amount of lag time. This shows that there may be large-scale eddies at moving at low frequencies across a landscape. However, there are periods in between the correlated time frames that do not appear to be correlated, which suggests that these large-scale motions are not predictable simply based on time.

4.3 Meteorological Impact on CO_2 Fluxes

Despite meteorological conditions being relatively similar between days and measurement sites, the subtle differences in synoptic conditions could make horizontal transport of CO_2 significant and vary for each day. Furthermore, weak mixing of the boundary layer could contribute to strong vertical gradients in CO_2, which would explain the large differences in surface CO_2 fluxes from the Picarro measurements compared to the tall tower measurements. Vertical mixing of CO_2 outweighs the uptake of CO_2 by vegetation for days three and four, but the uptake of CO_2 by vegetation may dominate for day five. An alternative explanation for the large positive surface flux values from the Picarro could be that the air masses that we were "chasing" had abnormally high CO_2 concentrations that outweighed uptake by vegetation. This is further confirmed if there was weak mixing.

The fact that the Picarro measured large positive carbon sources at the surface almost every day signifies weak mixing in the boundary layer, which allows for the presence of strong vertical gradients of CO_2. This suggests that 2 m measurements of CO_2 better represent the impact of horizontal transport--i.e. windiness--on CO_2 concentrations compared to the WLEF 122 m eddy flux measurements.

5. Conclusions and Future Directions

Our observations of varying CO_2 concentration over different terrain was likely due to meteorological forcings rather than vegetation. A negative flux was observed on Day 5 when dominant vegetation was aspen, but fluxes on all other days were positive. Although it is possible that logged piles of aspen could contribute to CO_2 production, it is unlikely that vegetation would have been emitting CO_2 in peak summer months, and in the late morning hours (9 am to 11 am). Typical fluxes from vegetation are also in a much lower range than what we observed (i.e., -20 to 20 $\mu molm^{-2}s^{-1}$ rather than -49 to 165).

The negative flux on Day 5 also suggests that vegetation CO_2 uptake dominates vertical mixing, whereas weak mixing and strong vertical gradients dominate on all other days. We also considered the alternative that the air masses that our team was “chasing” had abnormally high CO_2 concentrations. However, this is unlikely given the amount of data that was collected.

The wavelet analysis showed that there was indeed a correlation between upwind and downwind CO_2 concentrations each day. It is important to note that correlations between the data last for only a few minutes, followed by periods of time with no correlation. This suggests that there are large-scale eddies that move through the area, potentially causing vertical mixing, or that occur as a result of vertical mixing, at random times throughout the day.

In the future, CO_2 concentration measurements should be taken at the ground surface continuously in order to compare to tall tower measurements over a longer period of time. This would allow large eddies at low frequencies to be captured more efficiently as they move through a landscape.

References

Bakwin, P.S., K.J. Davis, C. Yi, S.C. Wofsy, J.W. Munger, L. Haszpra & Z. Barcza, 2004: Regional Carbon Dioxide Fluxes from Mixing Ratio Data, *Tellus B: Chemical and Physical Meteorology*, **56**:4, 301-311, DOI: 10.3402/tellusb.v56i4.16446.

Davis, K. J., P. S. Bakwin, C. Yi, B. W. Berger, C. Zhao, R. M. Teclaw, and J. G. Isebrands, 2003: The annual cycle of CO_2 and H_2O exchange over a northern mixed forest as observed from a very tall tower. *Global Change Biol*, **9,** 1278–1293.

Hurwitz, M.D., D.M. Ricciuto, P.S. Bakwin, K.J. Davis, W. Wang, C. Yi, and M.P. Butler, 2004: Transport of Carbon Dioxide in the Presence of Storm Systems over a Northern Wisconsin Forest. *J. Atmos. Sci.*, **61**, 607–618, https://doi.org/10.1175/1520-0469(2004)061<0607:TOCDIT>2.0.CO;2.

Wang, J.-W., A.S. Denning, L. Lu, I.T. Baker, K.D. Corbin, and K.J. Davis, 2007: Observations and Simulations of Synoptic, Regional, and Local Variations in Atmospheric CO2, *J. Geophys. Res.*, **112**, D04108, DOI: 10.1029/2006JD007410.

Yi, C., K. J. Davis, B. W. Berger, and P. S. Bakwin, 2001: Long-term observations of the dynamics of the continental planetary boundary layer. J. *Atmos. Sci*, **58**, 1288–1299.

Appendix

Figure 1: Map of Windsonde Paths

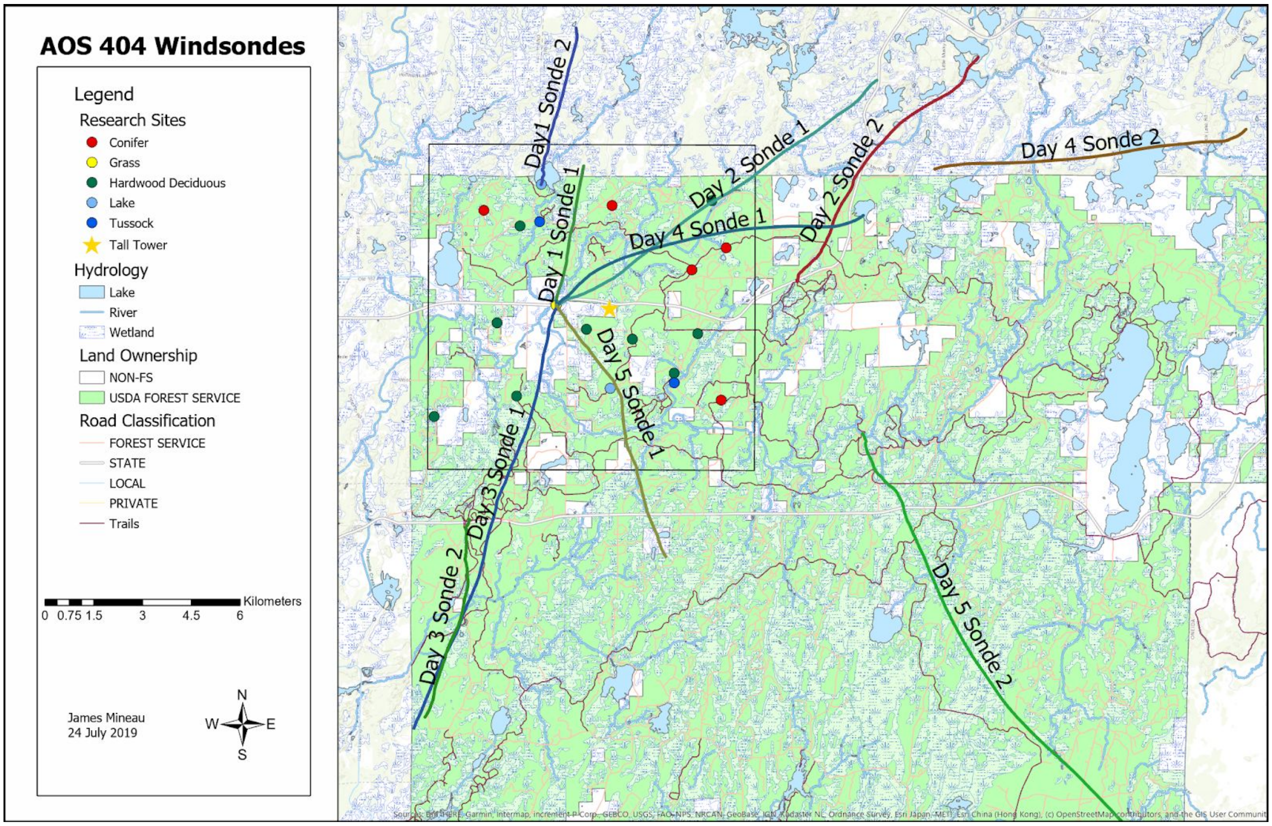

Figure 2: Map of Picarro "Paths"

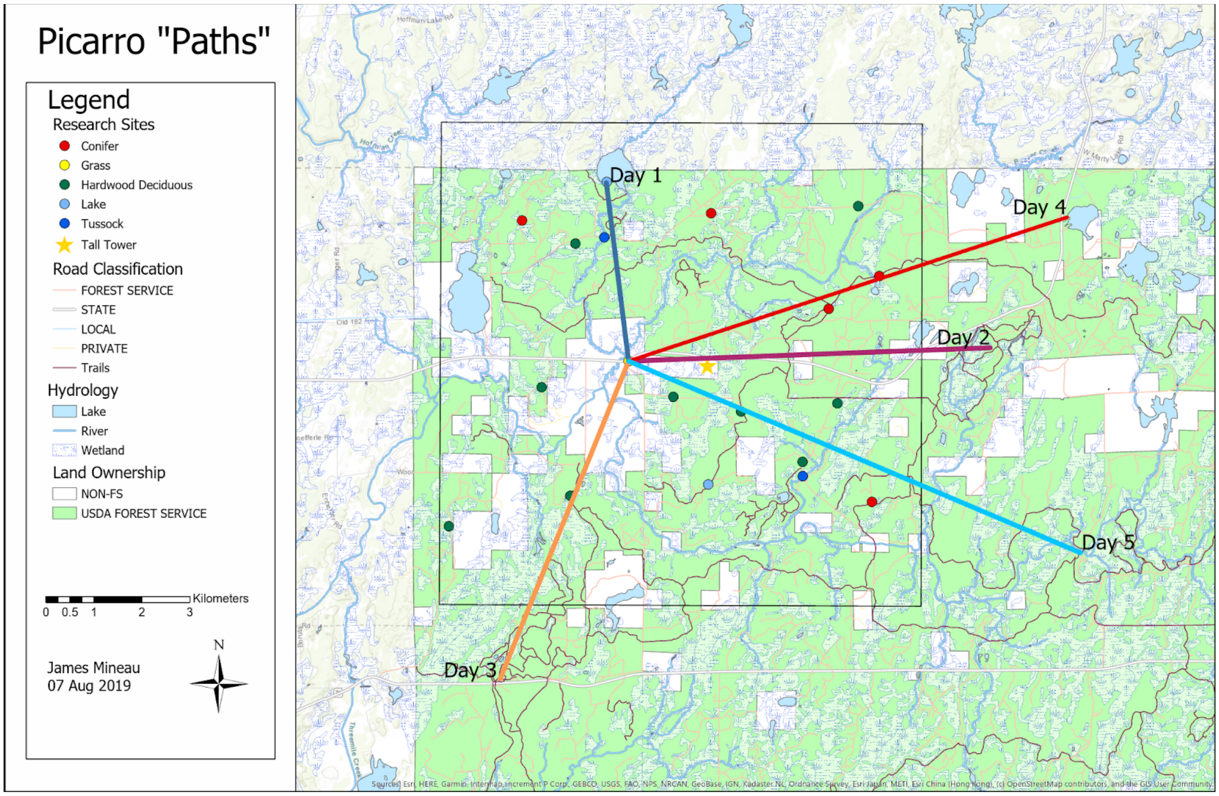

Figure 3: Vegetation Between First and Second Launch Sites

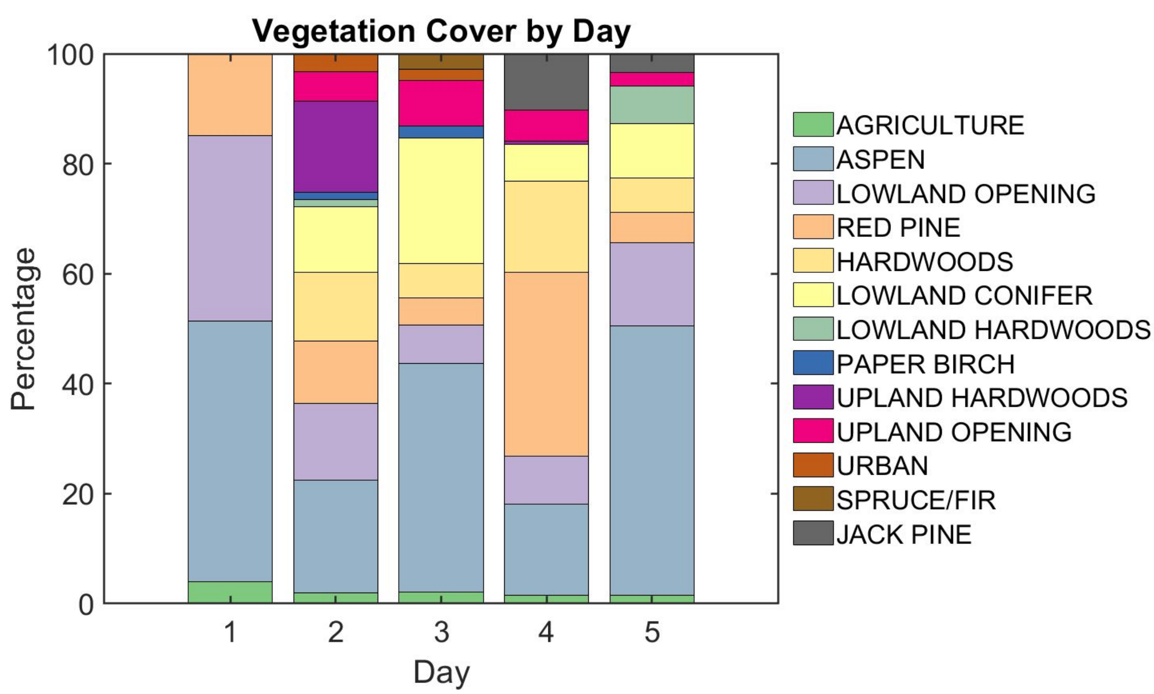

Interactive Vegetation + CO_2 ArcGIS Map:

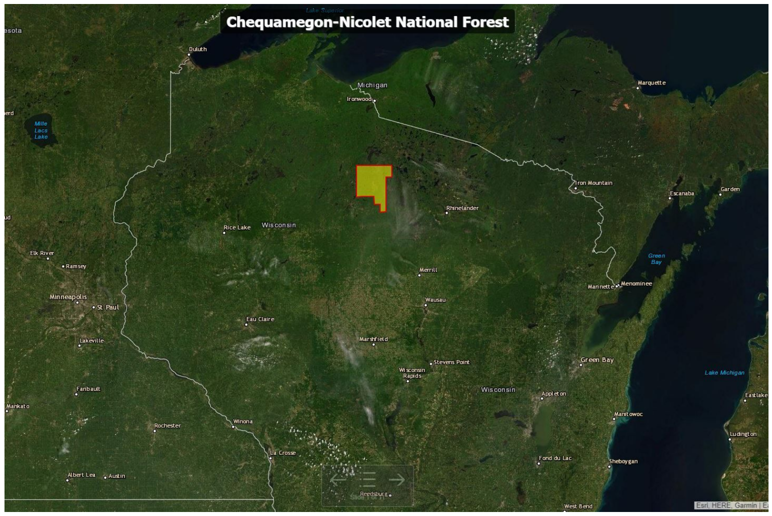

https://arcg.is/1CyHKX

Figures 4-8: Wavelet Coherence of WLEF 396m to Picarro Data

For wavelets, right-arrows signal that the data is in-phase. Left-arrows signal that data is anti-phase, down-arrows signal that WLEF tall tower concentrations lead Picarro data by 90°, and up-arrows signals that WLEF tall tower concentrations lead Picarro data by 270°. Data outside the white dashed line, or “cone of influence”, should not be considered because these data could be impacted by edge effects.

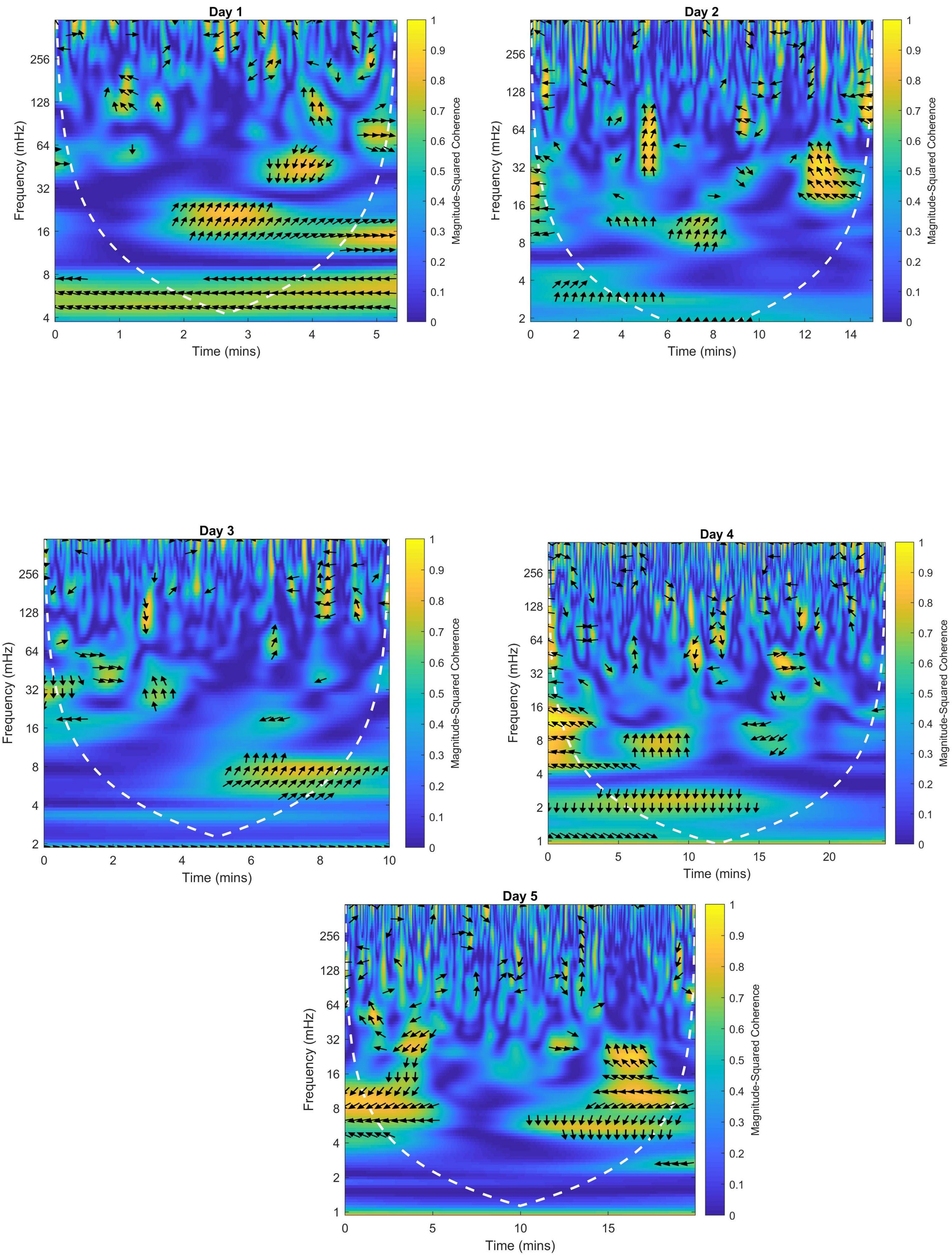

Day 1
Day 2
Day 3
Day 4
Day 5
Frequency (mHz)
Time (mins)
Magnitude-Squared Coherence
256
128
64
32
16
8
4
2
1
0
0.1
0.2
0.3
0.4
0.5
0.6
0.7
0.8
0.9
1

Figure 9: Potential Temperature Profiles

Shown below are potential temperature profiles calculated using temperature data from the windsondes. Potential temperature is given by $\theta(p) = T(\frac{p_0}{p})^{R_d/C_p}$ where p is the pressure at a given level in the atmosphere, p_0 is reference pressure, and T is temperature. It is used to detect the boundary layer height, which is signified by the temperature inversion. The boundary layer heights at each of our sites for Field Day 5 are marked by the dashed red line in the plots below. On the left is the vertical potential temperature profile at ISS and the right is at Smith Rapids Bridge. We can see that the boundary layer increased from just under 1100 m AGL at ISS to 1115 m AGL at Smith Rapids.

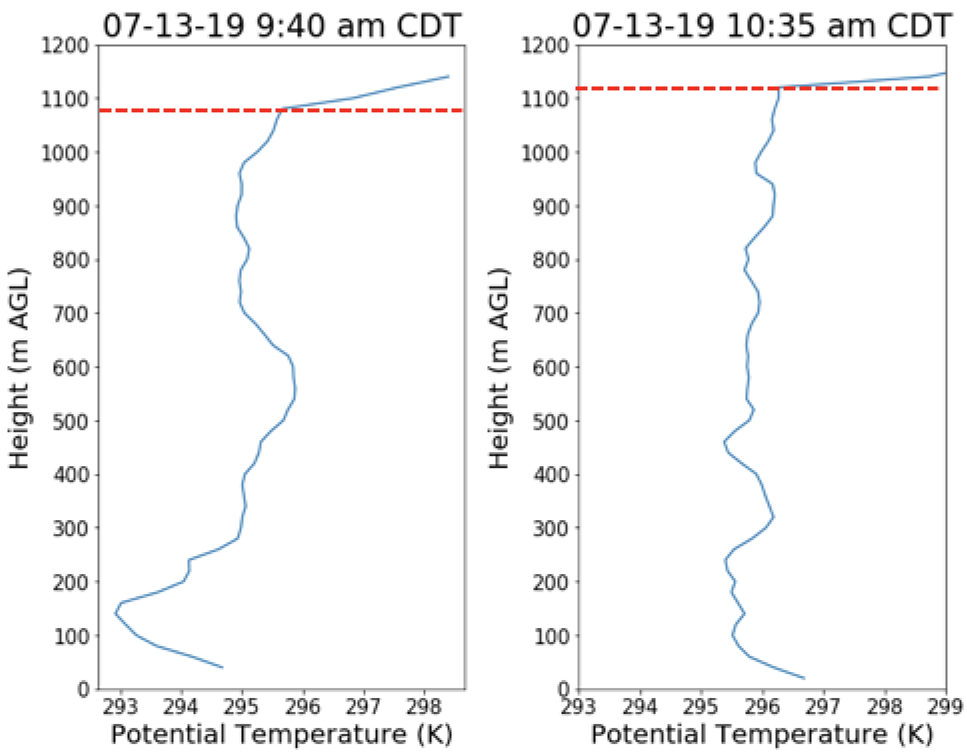

Figure 10: Day 1 Vegetation

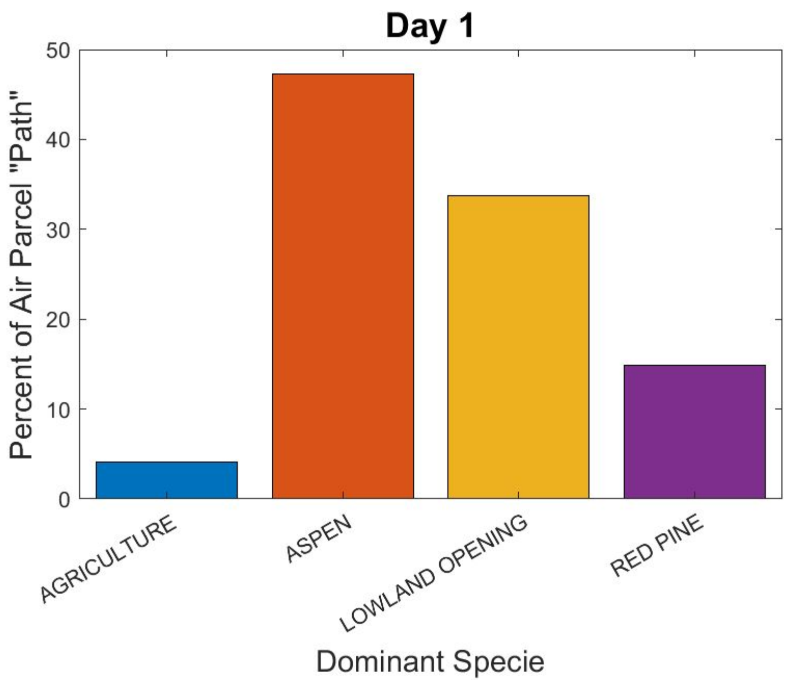

Figure 11: Day 2 Vegetation

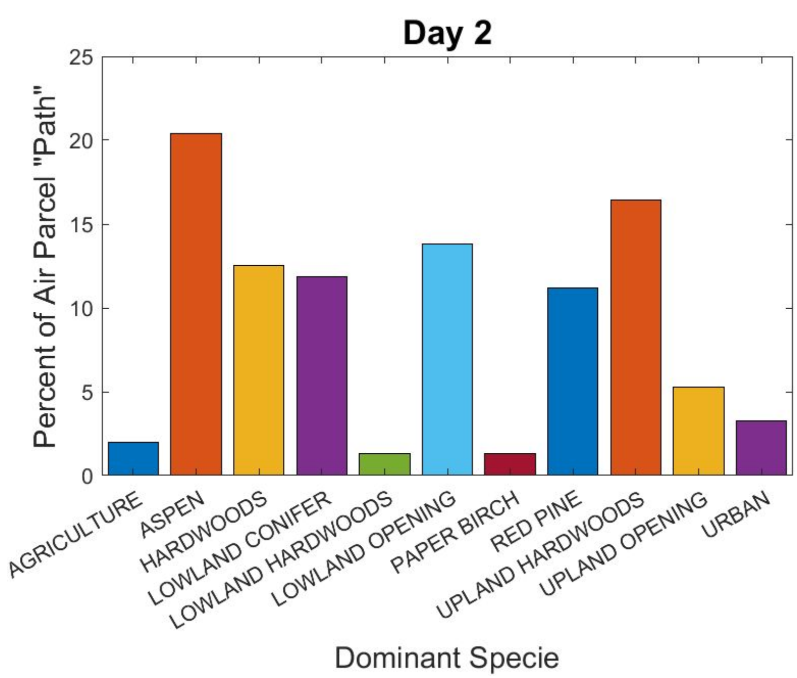

Figure 12: Day 3 Vegetation

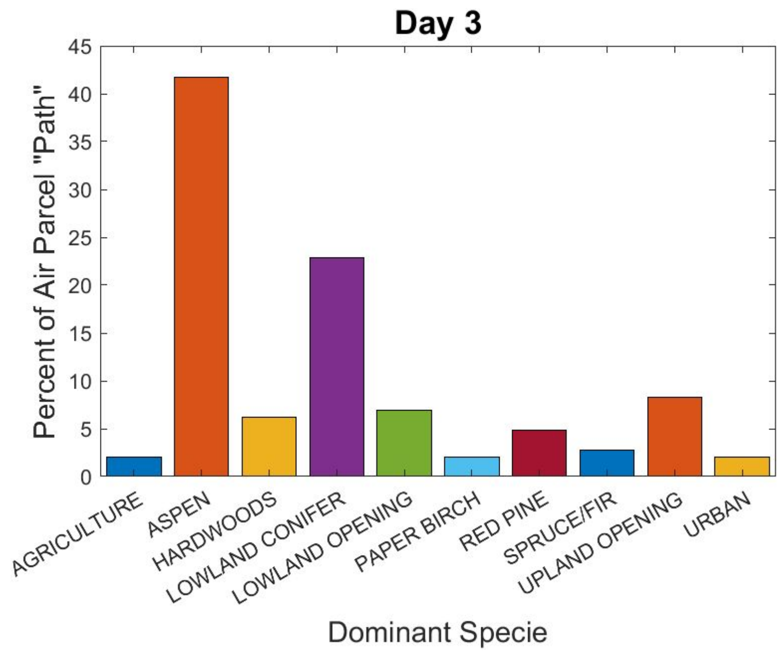

Figure 13: Day 4 Vegetation

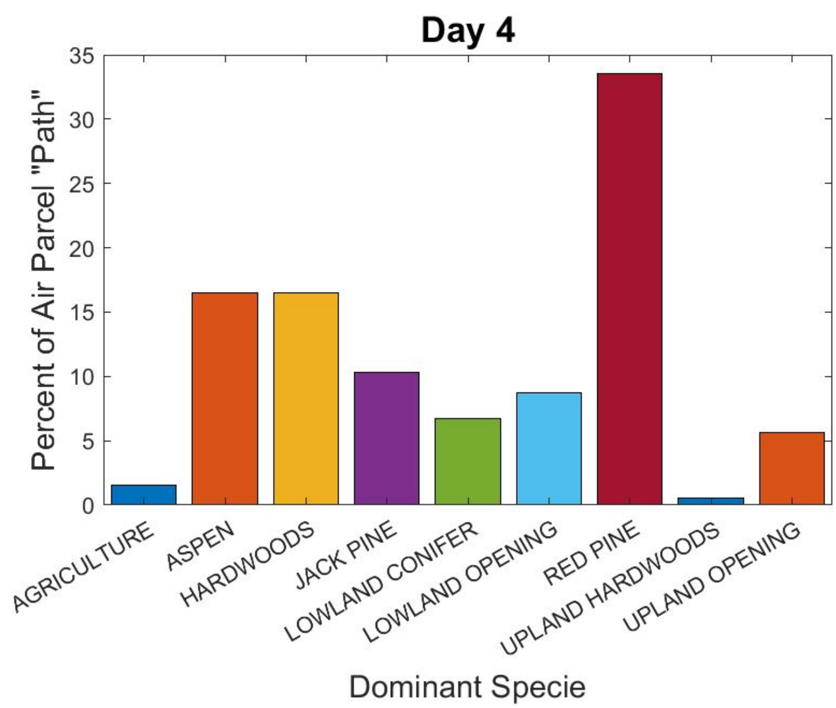

Figure 14: Day 5 Vegetation

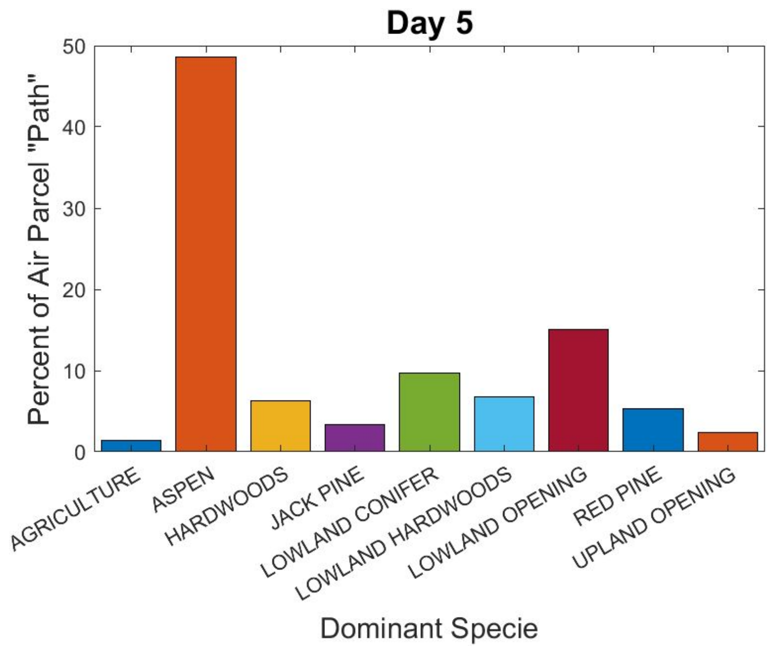

Figures 15-24: Wind Speed

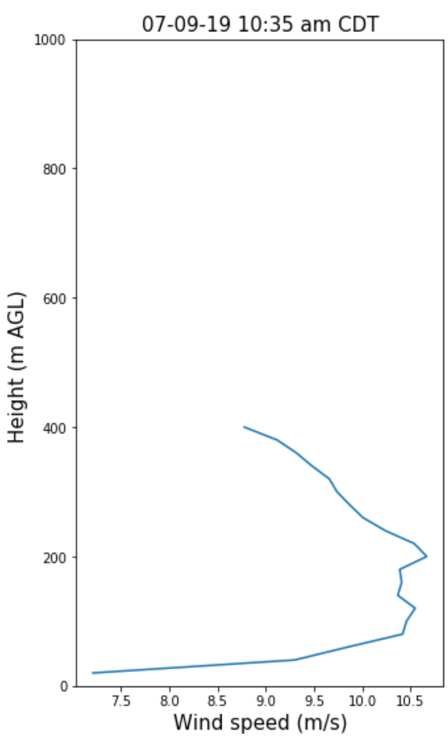

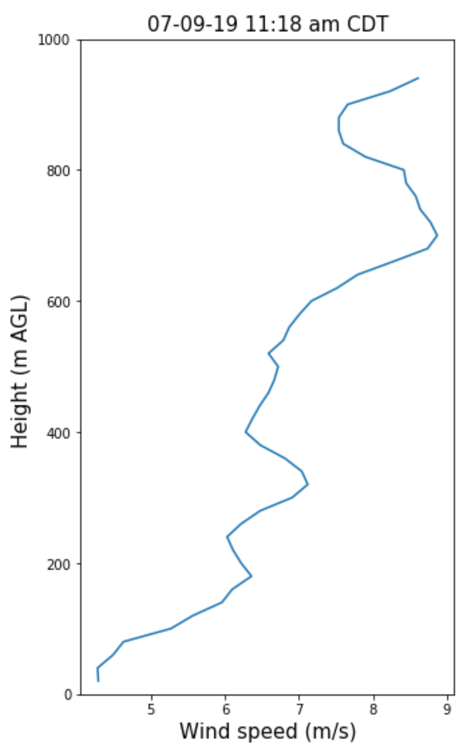

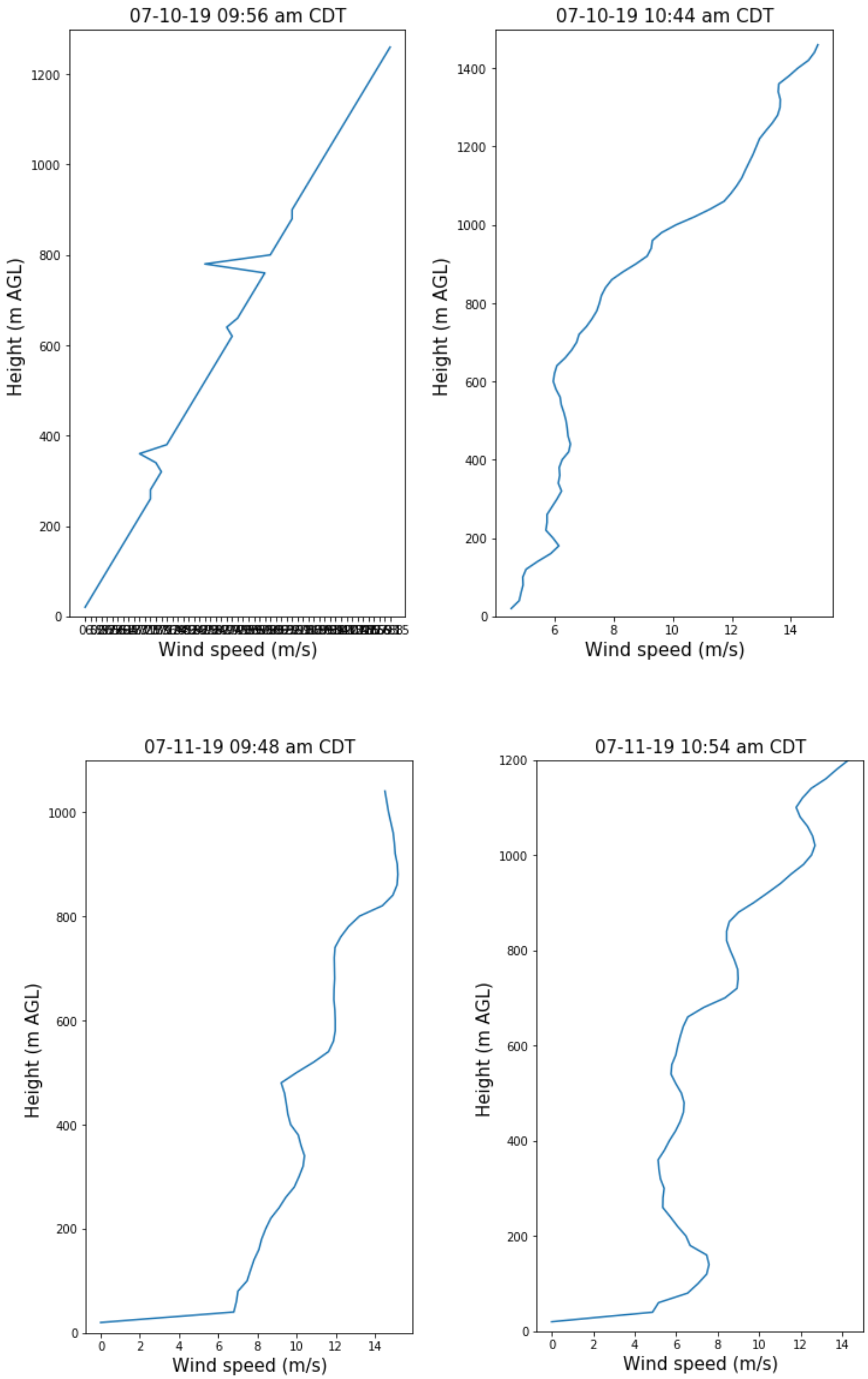
07-10-19 09:56 am CDT
Height (m AGL)
Wind speed (m/s)
0
200
400
600
800
1000
1200
07-10-19 10:44 am CDT
Height (m AGL)
Wind speed (m/s)
0
200
400
600
800
1000
1200
1400
6
8
10
12
14
07-11-19 09:48 am CDT
Height (m AGL)
Wind speed (m/s)
0
200
400
600
800
1000
0
2
4
6
8
10
12
14
07-11-19 10:54 am CDT
Height (m AGL)
Wind speed (m/s)
0
200
400
600
800
1000
1200
0
2
4
6
8
10
12
14

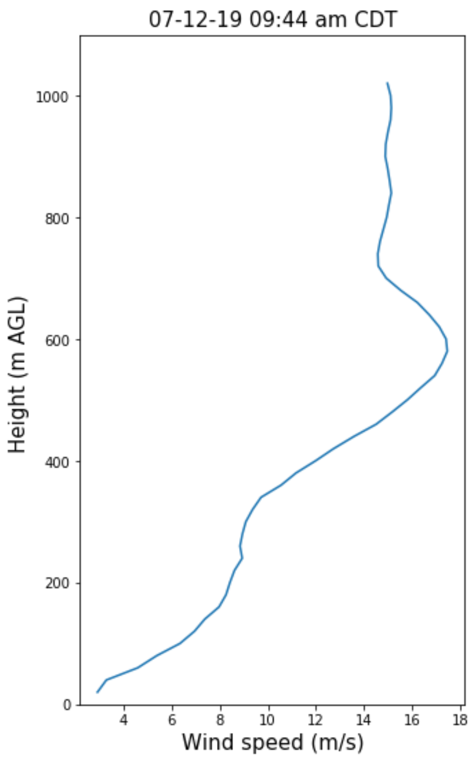
07-12-19 09:44 am CDT
Height (m AGL)
Wind speed (m/s)
0
200
400
600
800
1000
4
6
8
10
12
14
16
18

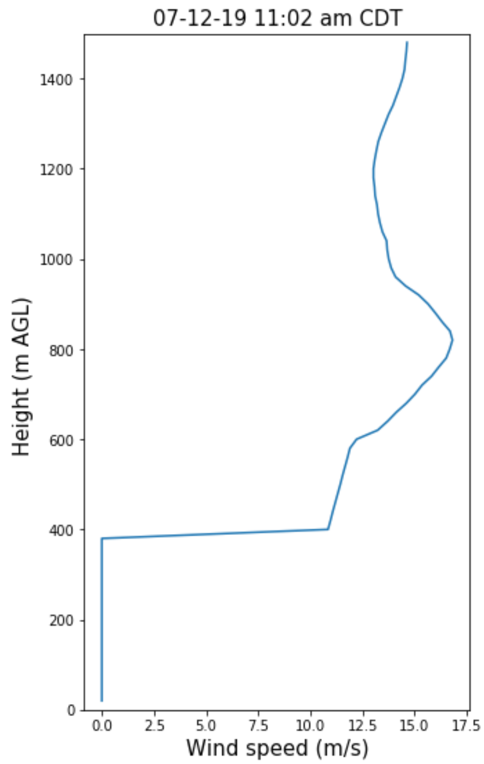
07-12-19 11:02 am CDT
Height (m AGL)
Wind speed (m/s)
0
200
400
600
800
1000
1200
1400
0.0
2.5
5.0
7.5
10.0
12.5
15.0
17.5

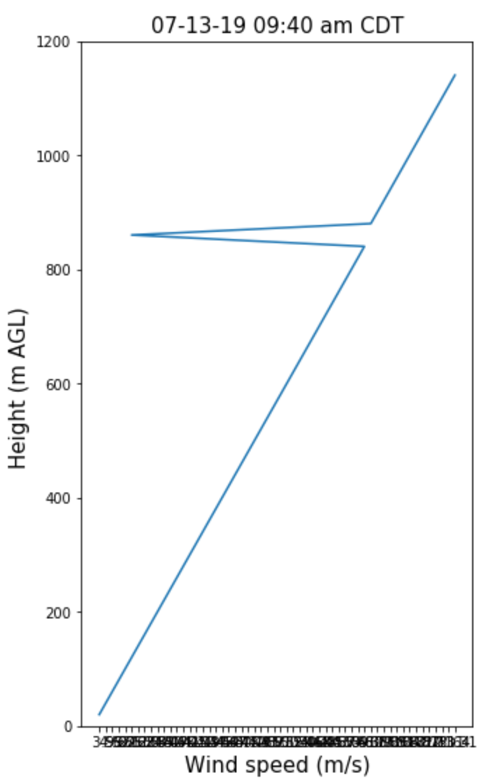
07-13-19 09:40 am CDT
Height (m AGL)
Wind speed (m/s)
0
200
400
600
800
1000
1200

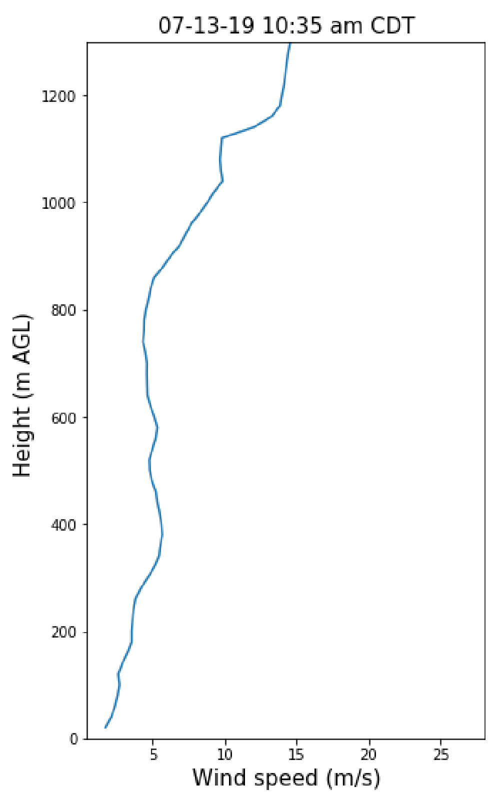
07-13-19 10:35 am CDT
Height (m AGL)
Wind speed (m/s)
0
200
400
600
800
1000
1200
5
10
15
20
25

Wind speed and direction were used to determine a second site to launch our windsondes. We followed the path of the wind and chose a location in that general direction. Our original plan was to follow the same air mass to a second location, but we quickly realized that the wind moved much faster than we could catch up with.

Figures 25-32: Potential Temperature Profiles

Below are the potential temperature profiles for days 1-4 of the field campaign. The plots on the left are from ISS and on the right are profiles from the second launch site, which varied each day.

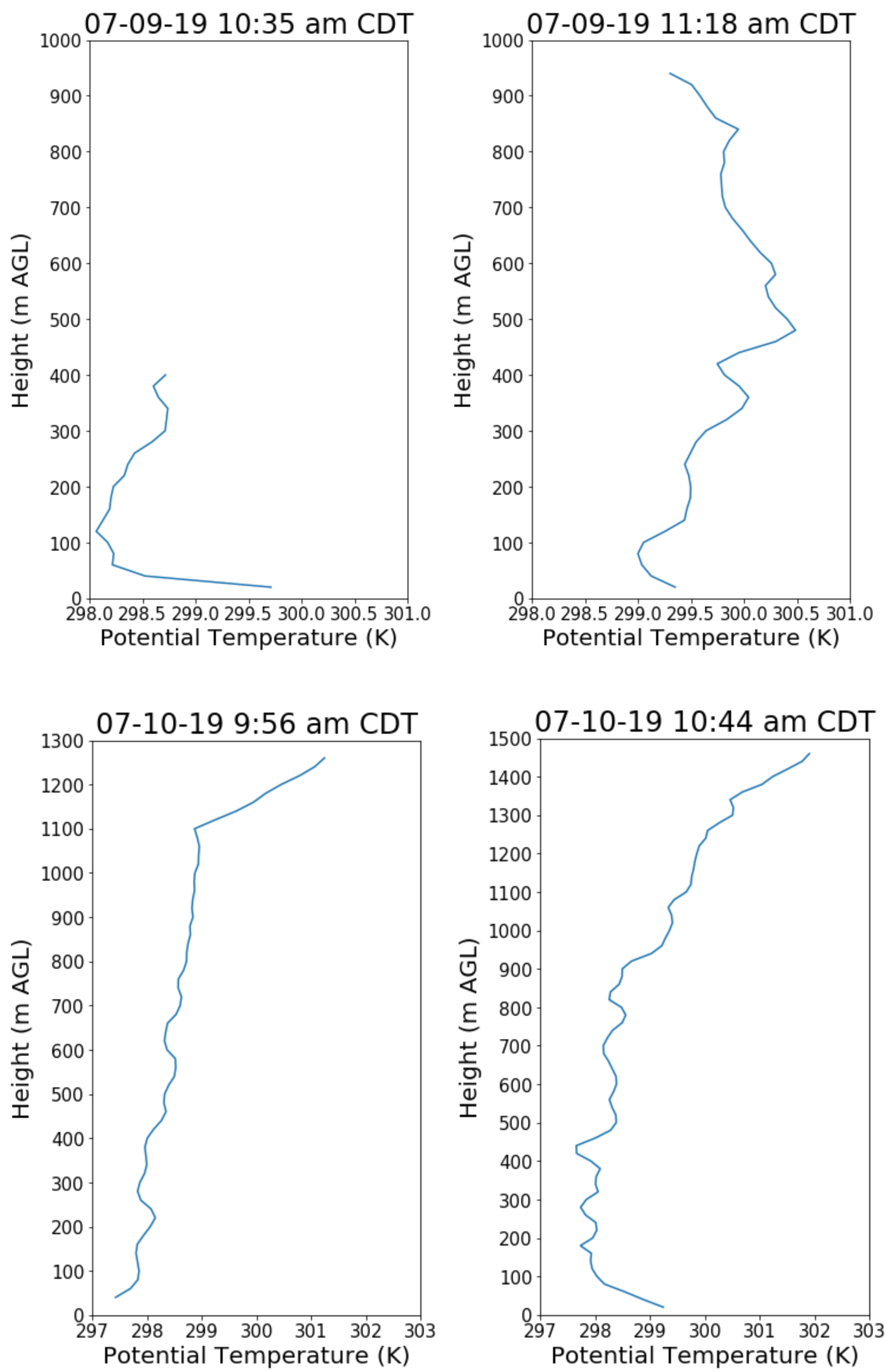
07-09-19 10:35 am CDT
Height (m AGL)
Potential Temperature (K)
0
100
200
300
400
500
600
700
800
900
1000
298.0
298.5
299.0
299.5
300.0
300.5
301.0
07-09-19 11:18 am CDT
Height (m AGL)
Potential Temperature (K)
0
100
200
300
400
500
600
700
800
900
1000
298.0
298.5
299.0
299.5
300.0
300.5
301.0
07-10-19 9:56 am CDT
Height (m AGL)
Potential Temperature (K)
0
100
200
300
400
500
600
700
800
900
1000
1100
1200
1300
297
298
299
300
301
302
303
07-10-19 10:44 am CDT
Height (m AGL)
Potential Temperature (K)
0
100
200
300
400
500
600
700
800
900
1000
1100
1200
1300
1400
1500
297
298
299
300
301
302
303

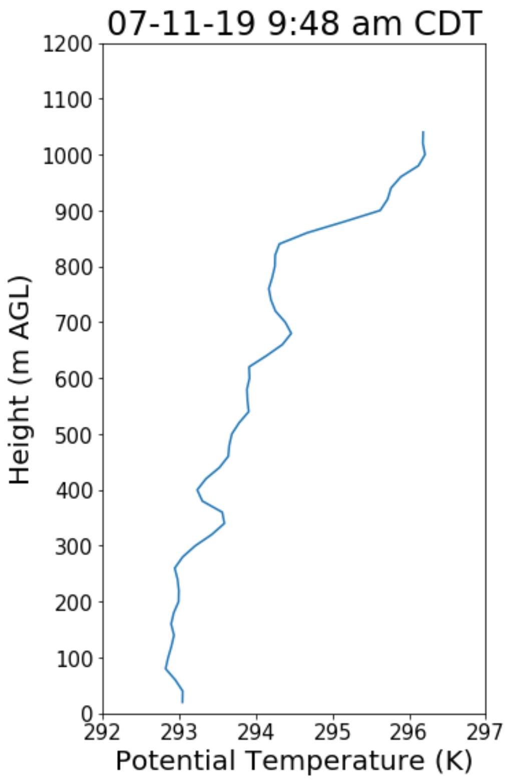
07-11-19 9:48 am CDT
Height (m AGL)
0
100
200
300
400
500
600
700
800
900
1000
1100
1200
292
293
294
295
296
297
Potential Temperature (K)

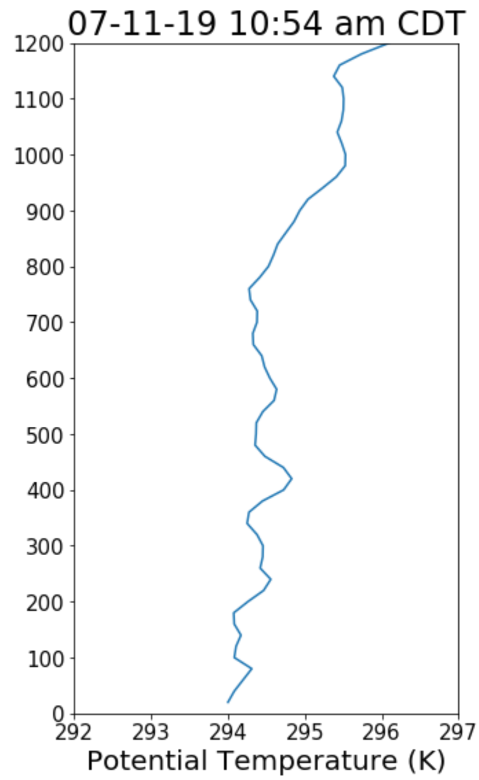
07-11-19 10:54 am CDT
0
100
200
300
400
500
600
700
800
900
1000
1100
1200
292
293
294
295
296
297
Potential Temperature (K)

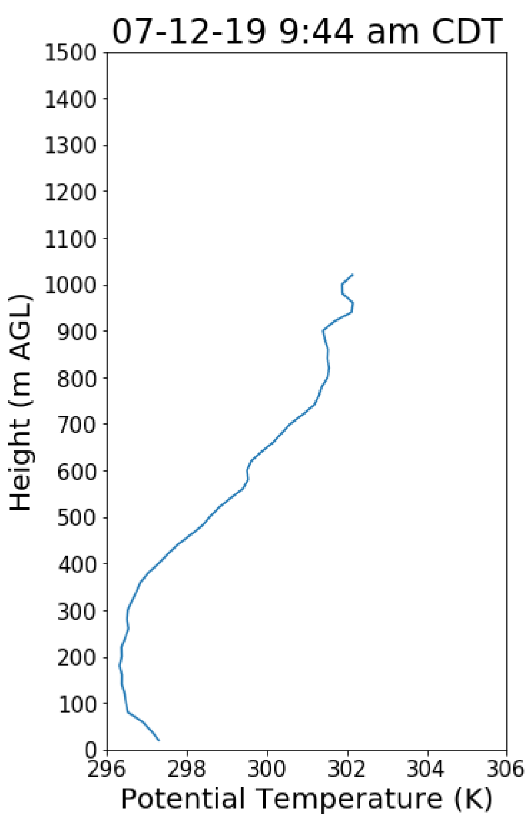
07-12-19 9:44 am CDT
Height (m AGL)
0
100
200
300
400
500
600
700
800
900
1000
1100
1200
1300
1400
1500
296
298
300
302
304
306
Potential Temperature (K)

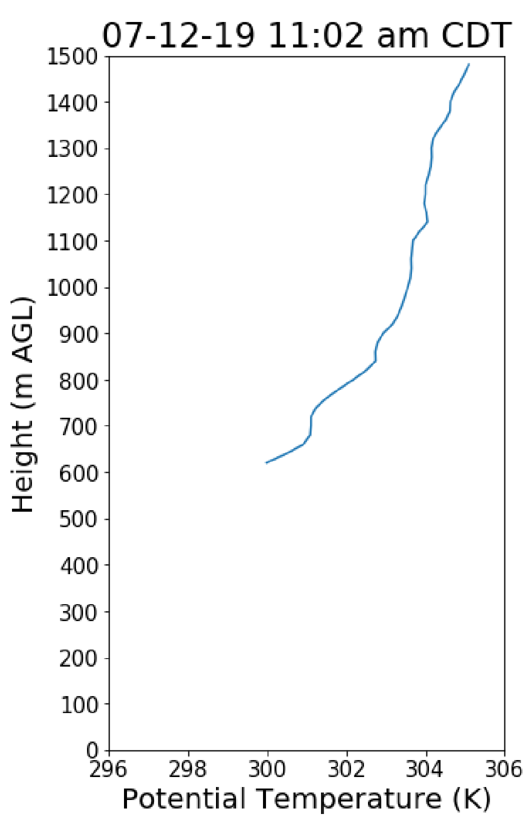
07-12-19 11:02 am CDT
Height (m AGL)
0
100
200
300
400
500
600
700
800
900
1000
1100
1200
1300
1400
1500
296
298
300
302
304
306
Potential Temperature (K)

Table 1: CO_2 Fluxes

Distance represents the linear distance between ISS and the second launch site. Time represents the time between launches. Average BLH represents the boundary layer heights from the first and second launches averaged together. BLH is measured in meters above ground level. WLEF tall tower concentrations are from the 122 m sensor. Picarro flux represents the change in CO_2 concentrations measured by the Picarro from the first to second launch sites using Equation 1. WLEF Flux represents the eddy flux of CO_2 at the 122 m sensor at 1500 UTC. Flux units are $\mu molm^{-2}s^{-1}$.

Day	Average BLH	Distance	Time (min)	Tair (°C)	WLEF Launch 1	WLEF Launch 2	Picarro Flux	WLEF Flux
1	1145.6 m	3750 m	43	21.7	388.6	389.2	164.8	-11.6
2	1175.0 m	7522 m	48	22.2	404.5	404.6	16.5	-8.7
3	1150.0 m	7093 m	66	17.8	397.3	395.8	142.5	-8.8
4	1125.0 m	9596 m	78	19.4	387.3	389.9	40.5	4.0
5	1112.5 m	10194 m	55	18.9	394.8	394.9	-48.9	-8.5